IOP Publishing Journal of Optics
J. Opt. **12** (2010) 035202 (5pp) doi:10.1088/2040-8978/12/3/035202

Domain patterns for quasi-phase matching in whispering-gallery modes

D Haertle

Institute of Physics, University of Bonn, Wegelerstraße 8, D-53115 Bonn, Germany

E-mail: haertle@uni-bonn.de

Received 14 July 2009, accepted for publication 8 October 2009
Published 20 January 2010
Online at stacks.iop.org/JOpt/12/035202

Abstract
Quasi-phase matching conditions for second-harmonic generation are analyzed for whispering-gallery modes. Several domain patterns, particularly those useful for resonators made of lithium niobate, are compared in terms of their effective nonlinear optical coefficients and spectral bandwidths. Only if the grating period at the circular surface of the resonator is monotonically increasing will the effective nonlinearity be independent of small variations of the properties of the resonator, such as the radius, and the offset between the domain pattern and the center of the resonator.

Keywords: QPM, SHG, whispering-gallery mode, WGM, $LiNbO_3$

(Some figures in this article are in colour only in the electronic version)

1. Introduction

Quasi-phase matched nonlinear optical effects in lithium niobate ($LiNbO_3$) crystals are widely used, e.g., for second-harmonic generation (SHG) [1–3] and optical parametric oscillation [4–6]. Quasi-phase matching (QPM) compensates the effect of the dispersion of the refractive index by inverting the sign of the nonlinear optical susceptibility when the pump beam and the signal beam get out of phase, which typically happens on the scale of 10 μm [7].

Whispering-gallery mode (WGM) resonators are round monolithic resonators, in which the light propagates around the equator, kept inside the dielectric material by total internal reflection [8]. In combination with WGM resonators efficient SHG was demonstrated at mW power levels [3], using conventional periodically poled lithium niobate (PPLN). In theory, a radially symmetric domain pattern would be best adapted to the circular form of the WGM resonator [9], and could lower the minimal pump power even further by more than one order of magnitude.

The radial patterns prove difficult to manufacture in $LiNbO_3$ with the standard lithographic poling method, since domain walls are not stable if they are not parallel to a crystallographic symmetry plane. In effect, the only implementation of a radial pattern in $LiNbO_3$ [10] was produced by a scanning technique known as 'calligraphic poling' [11]. Furthermore, with perfect radial poling the phase matching becomes very selective and the temperature of the resonators has to be controlled up to the order of mK.

It is thus desirable to reach a compromise between the highest nonlinearity and some tunability. With a chirp (or another deviation from periodicity) in the domain period 'seen' by the circulating light, one obtains phase matching for many pump frequencies in a given range. This is equivalent to some tunability in the resonator size or temperature at a fixed pump frequency. Also, since in WGM resonators the light propagates in a circle, the simplest domain patterns inherently show a strong chirp in the domain period.

2. SHG in doubly resonant cavities

For second-harmonic generation in WGMs two conditions have to be fulfilled: firstly, both the fundamental wave and its frequency-doubled form have to be modes of the resonator, and secondly, the phase matching condition has to be satisfied.

2.1. Double resonance

Let us assume that the second-harmonic frequency 2ω generated is resonant with the cavity. Then in general the pump frequency ω will be out of resonance, by a detuning $\Delta = |\omega - \tilde{\omega}|$ from the nearest resonance frequency $\tilde{\omega}$. The second-harmonic oscillation can still build up, if that detuning

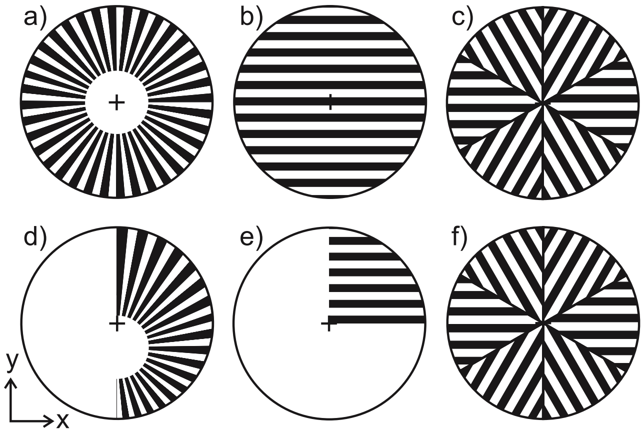

Figure 1. Domain patterns examined for SHG efficiency and bandwidth. (a) Radial; (b) PPLN; (c) 6-PPLN, i.e. six segments of PPLN; (d) half-radial; (e) quarter-PPLN; (f) optimized for $LiNbO_3$, i.e. equidistant on the circumference, as in (a) but with domain boundaries along the crystallographic axes. While in (c) the width of the stripes is constant, in (f) it is adapted for achieving the optimal pattern on the circumference. All the patterns can have an offset with respect to the center of the resonator, as illustrated by the example in (d).

is smaller than half of a linewidth [9], i.e. $\Delta < \gamma$, and we have

$$\frac{\Delta}{\gamma} = 2Q\left|\frac{\tilde{\omega}}{\omega} - 1\right| \tag{1}$$

where the quality factor Q for the fundamental wave relates to its linewidth via $Q = \omega/(2\gamma)$. Taking into account only the fundamental series of resonances ($q = 1$, $m = l$), the average detuning is $\langle\Delta\rangle = \omega/4 = c/(4nR)$, and $\langle\Delta\rangle/\gamma$ scales inverse proportionally to the radius R for a fixed Q. For $Q = 10^7$ and $\lambda_p = 1.5\ \mu$m, the detuning stays larger than γ for $R < 100$ cm. Therefore resonator forms [12] with a dense mode spectrum should be preferred, where $\langle\Delta\rangle = \gamma$ can be reached for $R \approx 1$ mm [9]. It is also possible to tune the temperature or another property which shifts the modes differently for different wavelengths, to achieve mode overlap.

2.2. Phase matching

While phase matching in microscopic WGM resonators can be achieved by compensating the material dispersion with the dispersion of the cavity modes [13], for macroscopic WGM resonators the same techniques are used as with free beams, the commonest being phase matching using birefringence and quasi-phase matching. In this paper we will concentrate on the latter, since it is the best choice for nonlinear optics with $LiNbO_3$ crystals, where PPLN is widely used.

The two simplest domain patterns (centered radial and linear patterns shown in figures 1(a) and (b)) have already been investigated in [9]. Here we analyze several more domain patterns, and account for among other things a possible shift of the center of the domain patterns with respect to the center of the resonator.

For QPM the spontaneous polarization is switched periodically after a distance $l_c = \pi/\Delta k$, where l_c is the coherence length and $\Delta k = k_{2\omega} - 2k_\omega$ is the mismatch of the wavevectors. The resulting domain period $\Lambda = 2l_c = 2\pi/\Delta k$ is optimal for light traveling straight through the crystal, perpendicular to the grating. In this case the effective nonlinear coefficient with QPM is $d_{eff} = \frac{2}{\pi}d_{sc}$, where d_{sc} is the effective coefficient of the single crystal, e.g. $d_{33} \approx 24$ pm V^{-1} for $LiNbO_3$ at $\lambda = 1550$ nm [14].

When the domain pattern seen by the beam is not periodic in the grating spacing $\Lambda = 2\pi/\Delta k$, as is, e.g., the case when the light is traveling in a circle inside a WGM resonator cut out of PPLN, the coefficient d_{eff} with QPM is

$$d_{eff} = \left|F_{pattern}\left(\frac{2\pi}{\Lambda}\right)\right| d_{sc} \tag{2}$$

where $F_{pattern}$ is the Fourier transform of the domain pattern $p(z) = \mathrm{sgn}(d(z))$ along one round-trip of length $L = 2\pi R$:

$$F_{pattern}(K) = \frac{1}{L}\int_0^L p(z)e^{-iKz}\,dz \tag{3}$$

evaluated at $K = 2\pi/\Lambda$. Here $d(z)$ is the nonlinear optical coefficient at the position z, which changes its sign at each domain boundary [15, 16].

When phase matching is satisfied the SHG efficiency for a single path through the crystal increases quadratically with $d_{eff}L$ and linearly with the pump intensity I_ω [17]. For WGMs we calculate the spectrum $d_{eff}(\Lambda)$ numerically in two ways: by directly solving equation (3) and by using the fast Fourier transform (FFT).

During manufacturing of a periodically poled resonator, some inaccuracies can occur: the domain pattern may have an offset (x_0, y_0) with respect to the center of the resonator, the radius of the resonator may be different from the design value, and the duty cycle DC of the pattern may deviate from its optimum value 0.5. Therefore all these parameters can be varied in the simulation.

2.3. Results and discussion

2.3.1. General observations. Unless otherwise stated, the simulations shown are calculated with the following parameters: $R = 2$ mm, $\Lambda_0 \approx 18\ \mu$m, $x_0 = y_0 = 0$, DC = 0.5, which correspond to typical parameters for SHG at $\lambda = 1550$ nm pump wavelength, and where Λ_0 is the grating spacing of the domain pattern[1]. Here Λ_0 is adjusted so that the ratio between the circumference and Λ_0 is $G = 2\pi R/\Lambda_0 = 700$, which ensures that the number of grating periods for the radial pattern is a whole one.

For a constant number of gratings G, the spectrum $d_{eff}(\Lambda)$ depends only on the ratio Λ/Λ_0. Therefore in all the figures the period Λ that is needed for phase matching is shown normalized to the actual grating period Λ_0 of the resonator.

The resolution of the FFT calculations in the Λ-space is limited to Λ_0/G, independently of the discretization chosen. This is because the fast Fourier transform gives d_{eff} only for an integer number of grating spacings Λ in one circumference. At these points, where $\Lambda = \Lambda_0$, $(1 + 1/G)\Lambda_0$, and so forth, the value coincides with equation (3). For a higher resolution one has to calculate the integral (3) directly, as is shown in figure 3.

[1] For the patterns with variable grating spacing (the ones in figures 1(a), (d) and (f)) Λ_0 is defined as the grating spacing at the radius R (see figure 2).

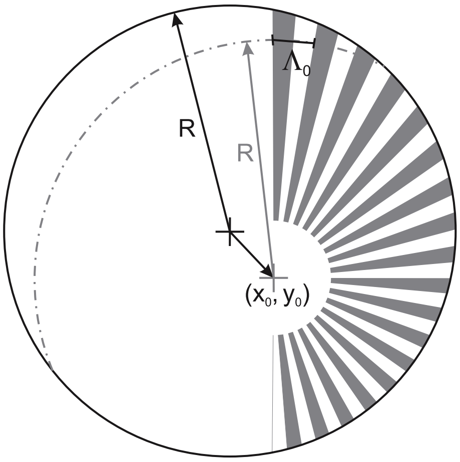

Figure 2. Illustration of the main parameters used in the simulations. The poling pattern is shifted by an offset (x_0, y_0) with respect to the center of the resonator, Λ_0 is the grating spacing, and R is the radius of the resonator.

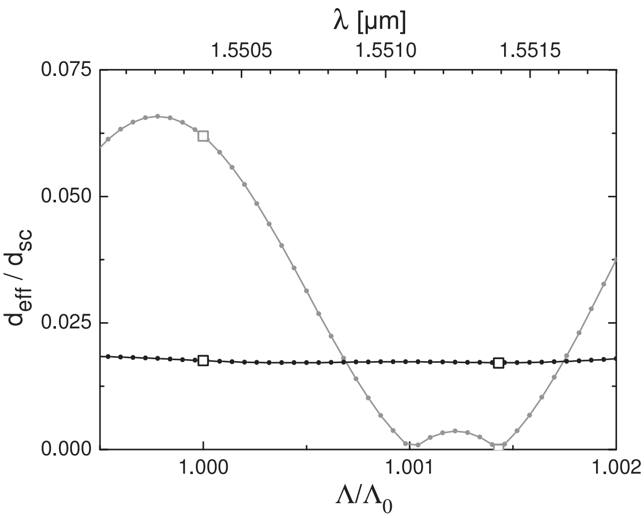

Figure 3. High resolution detail of the amplification spectrum, calculated for a PPLN pattern (gray) and a quarter-PPLN pattern (black). The small full points connected by straight lines are calculated with (3) while the large open squares are computed by using a FFT. The effective NLO coefficient is shown normalized to the single-crystal coefficient d_{sc} versus the mismatch Λ/Λ_0 on the bottom axis. The upper axis indicates the pump wavelength that requires the corresponding grating spacing for the case of a $LiNbO_3$ resonator with $\Lambda_0 = 18\ \mu$m.

A variation of the duty cycle has the same effect as in free-beam SHG: $d_{eff}/d_{eff,DC=0.5} = \sin(\pi DC)$.

2.3.2. PPLN and quarter-PPLN. With the PPLN pattern the light 'sees' a chirped grating, leading to contributions at all grating spacings $\Lambda > \Lambda_0$; see figure 4, where Fourier spectra of the PPLN and the quarter-PPLN patterns are compared. The peak values of d_{eff} are four times higher for PPLN, corresponding to the path that is phase matched being four times longer. However, second-harmonic

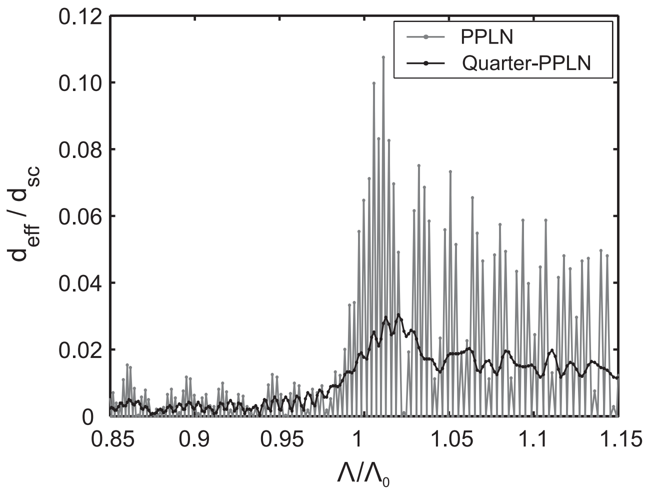

Figure 4. Normalized effective NLO coefficient versus the required grating spacing for a PPLN pattern (gray) and a quarter-PPLN pattern (black), calculated using a FFT. The FFT provides discrete points, which are connected in the figure by lines for ease of viewing. The real values of the effective NLO coefficient between these points depend on the parameters of the resonator, but they are mostly well approximated by straight lines (see figure 3). The x-axis is normalized to the grating spacing Λ_0.

light generated at the four equivalent regions of the PPLN pattern interferes coherently, possibly leading to an effectively vanishing nonlinearity at certain Λ, as seen in figure 4. Furthermore, in practice it is not possible to control the interference of equivalent regions in the resonator. Small variations of the radius of the resonator or an offset of the grating pattern with respect to the center of the resonator are inevitable during production. As can be seen in figure 5, a shift of $y_0 \approx 0.0022R \approx 4\ \mu$m of a PPLN pattern is enough to change the constructive interference into a destructive one (note that, at the same time, the adjacent destructive interference in figure 4 is changed into a constructive one). The quarter-PPLN pattern does not exhibit this behavior: this is because the grating period increases monotonically along the circumference, so there is no possibility of interference.

Another feature of the quarter-PPLN structure is that its large single-crystalline area can be used to tune the resonator by applying an electric field. When one has an asymmetry between the light path in $+z$ and $-z$ domains, an applied electric field can change the mean refractive index of the resonator via the Pockels effect. With a refractive index change $\Delta n = -n^3 r E/2$ given by the electric field E and the electro-optic coefficient r in a single-crystalline domain, the refractive index change averaged over the circumference of the resonator is $\overline{\Delta n} = \Delta n(1 - f_{pat})$, where f_{pat} is the fraction of the circumference covered by a domain pattern, i.e. 1/4 for the quarter-PPLN and $f_{pat} = 1$ for PPLN. The change of the resonance frequency is linear in $\overline{\Delta n}$ to a first approximation [9]. But due to the different values of n and r at ω and 2ω, the two frequencies will be changed differently: if without field one has the double resonance with the modes $(q_\omega, l_\omega, m_\omega)$ and $(q_\omega, l_{2\omega}, m_{2\omega})$, then with the quarter-PPLN pattern $(q_\omega, l_\omega, m_\omega)$ would be resonant with $(q_{2\omega}, l_{2\omega}+1, m_{2\omega})$

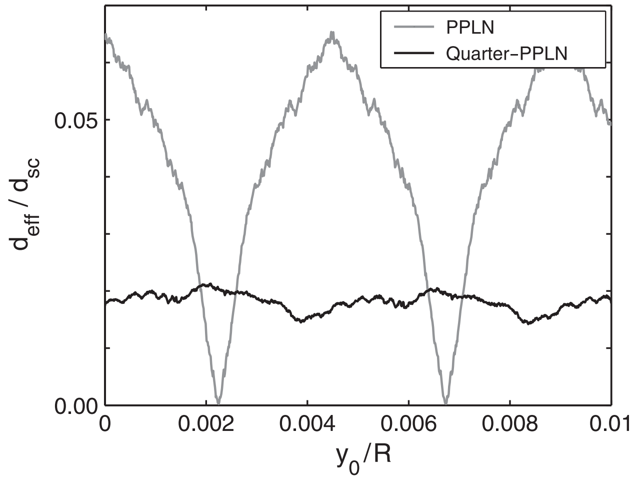

Figure 5. Normalized effective NLO coefficient at $\Lambda = \Lambda_0$ versus a small shift of the pattern along the y-axis.

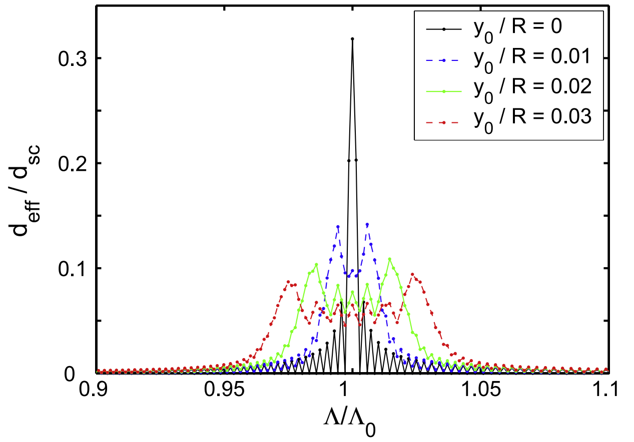

Figure 6. Normalized effective NLO coefficient versus the required grating spacing for a half-radial pattern, calculated using a FFT. The center of the domain pattern is shifted by an offset y_0 with respect to the center of the resonator.

at $E = 5.2$ kV mm^{-1}. This means that with this electric field difference one can always get double resonance, even in the case where the resonator has just a single mode per free spectral range. In practice one has a dense mode spectrum and a much smaller electric field is sufficient. One can also shift the refractive index by changing the temperature. This has the advantage of working with all domain structures. To the above field there corresponds a temperature change of 8 K according to the refractive index data in [18] and the thermal expansion data in [19].

2.3.3. Radial and half-radial. For a perfect radial pattern we have $d_{eff} = 2d_{sc}/\pi \approx 0.64d_{sc}$ at Λ_0, while the effective nonlinearity is zero for $\Lambda \neq \Lambda_0$ [9]. The maximal nonlinearity $d_{eff}(\Lambda_0)$ is much higher than for the patterns of section 2.3.2, since the right grating period is present on the whole circumference. Figure 6 gives the spectrum for the half-radial pattern, for different offsets y_0 of the center of the domain pattern with respect to the center of the resonator. For $y_0 = 0$ we get $d_{eff} = d_{sc}/\pi$ as the peak nonlinearity, while a non-zero offset gives an approximately linear chirp in the grating period, leading to a top-hat-like spectrum, centered around the original grating Λ_0. The width is inversely proportional to $d^2_{eff}(\Lambda_0)$ since the integral

$$\int d^2_{eff}(\Lambda)\,\mathrm{d}\Lambda = \frac{\Lambda_0^2}{L}\left(\frac{2}{\pi}f_{pat}d_{sc}\right)^2 \tag{4}$$

going over the 'peak' at Λ_0 is an invariant, valid for all patterns. In that respect a specific pattern just determines how the nonlinearity $d^2_{eff}(\Lambda)$ is distributed around Λ_0, and the half-radial pattern with offset distributes it more or less uniformly. For the full radial pattern with an offset we get the same form, but with interferences similarly to those in figure 4 for PPLN.

2.3.4. Optimized for $LiNbO_3$. Since the radial patterns prove difficult to manufacture in $LiNbO_3$, we investigate related patterns obeying the threefold crystallographic symmetry of this material (point group $3m$). The easiest approximation consists of six equivalent pieces of equidistant PPLN, as drawn in figure 1(c). This pattern, labeled as 6-PPLN, has a maximal d_{eff} three times higher than that of PPLN; see figure 7. The nonlinearity is effectively concentrated between Λ_0 and $1.15\Lambda_0$ (figure 8(b)), which is more than enough for applications. This concentration comes from the fact that in contrast to the case for the PPLN pattern the maximal period on the resonator's circumference is limited to $\Lambda_0/\cos 30°$. Figure 8 shows the nonlinearity when the pattern is shifted by less than Λ_0, for larger shifts the result being similar for this pattern.

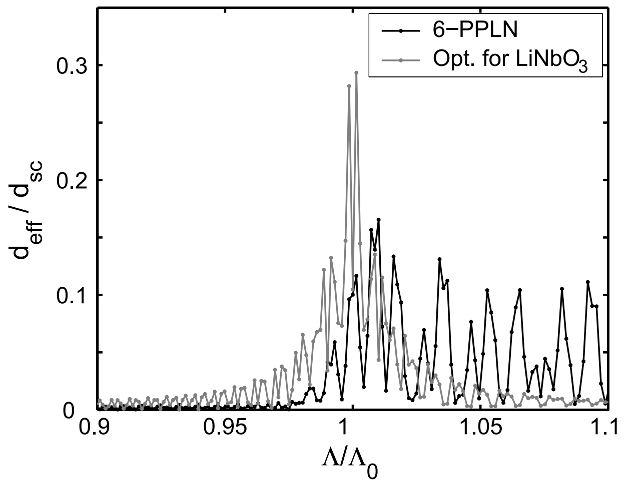

Figure 7. Normalized effective NLO coefficient versus the required grating spacing for a 6-PPLN pattern (black) and a pattern optimized for $LiNbO_3$ (gray), both with an offset of $(x_0/R, y_0/R) = (0.02, 0.02)$.

An even better approximation would be to vary the grating spacing such that on the circumference it does coincide with the radial pattern, yielding the pattern in figure 1(f). Without offset its spectrum is identical to that of the radial pattern, $d_{eff} = \frac{2}{\pi}d_{sc}$ at Λ_0, and zero for $\Lambda \neq \Lambda_0$, while figure 7 shows

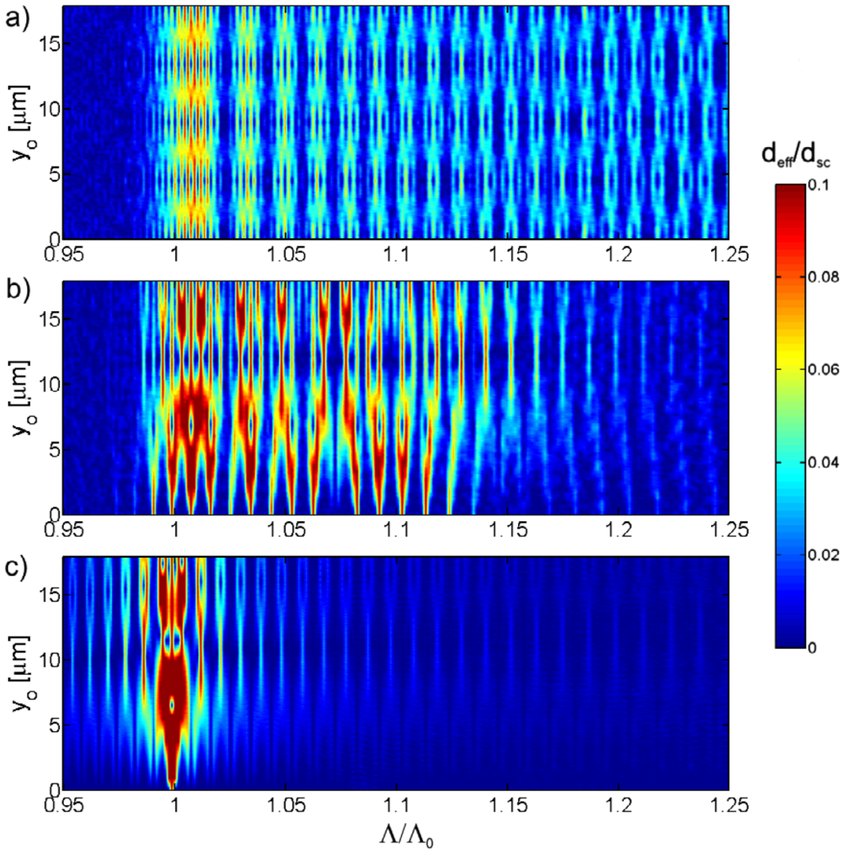

Figure 8. Normalized effective NLO coefficient versus the grating spacing and the offset in the y-direction for (a) PPLN, (b) 6-PPLN and (c) a pattern optimized for $LiNbO_3$.

the spectrum for an offset of $(x_0/R, y_0/R) = (0.02, 0.02)$. Also with offset the nonlinearity is well concentrated around Λ_0; see figure 8(c). For large offsets the spectrum spreads out at approximately half the speed of the radial patterns.

3. Conclusions

The conditions for quasi-phase matching in WGMs were analyzed in detail, and six poling patterns for $LiNbO_3$ resonators were compared in terms of effective nonlinearity and design tolerances. The efficiency at low light intensity of the standard PPLN pattern can be increased by approximately one order of magnitude by periodically poling along all three equivalent axes. At high light intensity a smaller nonlinearity is sufficient for good efficiency and it can be advantageous to keep single-domain regions, resulting in a smoother spectrum and the possibility of using an electric field to tune the resonator.

Acknowledgments

I thank K Buse and I Breunig for valuable discussions. Financial support by the DFG (FOR 557) and the Deutsche Telekom AG is gratefully acknowledged.

References

[1] Miller G D, Batchko R G, Tulloch W M, Weise D R, Fejer M M and Byer R L 1997 *Opt. Lett.* **22** 1834–6
[2] Fonseca Campos J, Wang Y, Chen B, Xu C Q, Yang S Q, Ponomarev E A and Bao X Y 2006 *J. Lightwave Technol.* **24** 3698–708
[3] Ilchenko V S, Savchenkov A A, Matsko A B and Maleki L 2004 *Phys. Rev. Lett.* **92** 043903
[4] Bosenberg W R, Drobshoff A, Alexander J I, Myers L E and Byer R L 1996 *Opt. Lett.* **21** 1336–8
[5] Breunig I, Kiessling J, Knabe B, Sowade R and Buse K 2008 *Opt. Express* **16** 5662–6
[6] Arizmendi L 2004 *Phys. Status Solidi* a **201** 253–83
[7] Fejer M M, Magel G A, Jundt D H and Byer R L 1992 *IEEE J. Quantum Electron.* **28** 2631–54
[8] Matsko A B and Ilchenko V S 2006 *IEEE J. Sel. Top. Quantum Electron.* **12** 3–14
[9] Ilchenko V S, Matsko A B, Savchenkov A A and Maleki L 2003 *J. Opt. Soc. Am.* B **20** 1304–8
[10] Mohageg M, Strekalov D, Savchenkov A, Matsko A, Ilchenko V and Maleki L 2006 *Proc. SPIE* **6101** 61010Q
[11] Mohageg M, Strekalov D V, Savchcnkov A A, Matsko A B, Ilchenko V S and Maleki L 2005 *Opt. Express* **13** 3408–19
[12] Ilchenko V S, Savchenkov A A, Matsko A B and Maleki L 2003 *Proc. SPIE* **4969** 195–206
[13] Carmon T and Vahala K J 2007 *Nat. Phys.* **3** 430–5
[14] Seres J 2001 *Appl. Phys.* B **73** 705–9
[15] Zhang C, Zhu Y, Zhu S and Ming N 2001 *Ferroelectrics* **253** 231–8
[16] Norton A H and de Sterke C M 2004 *Opt. Express* **12** 841–6
[17] Yariv A and Yeh P 2007 *Photonics* (Oxford: Oxford University Press)
[18] Jundt D H 1997 *Opt. Lett.* **22** 1553–5
[19] Taylor D 2002 *Properties of Lithium Niobate* (London: Inspec) chapter (Thermal Expansion Coefficients of $LiNbO_3$) pp 73–7